FEBS Letters 582 (2008) 3359–3366

Pyruvate uptake is inhibited by valproic acid and metabolites in mitochondrial membranes

Cátia C.P. Aires[a], Graça Soveral[b], Paula B.M. Luís[a], Herman J. ten Brink[c], Isabel Tavares de Almeida[a], Marinus Duran[d], Ronald J.A. Wanders[d], Margarida F.B. Silva[a,*]

[a] *iMED.UL, Centro de Patogénese Molecular, Faculdade de Farmácia da Universidade de Lisboa, Av. Prof. Gama Pinto, 1649-003 Lisboa, Portugal*
[b] *REQUIMTE, Departamento de Química, FCT, Universidade Nova de Lisboa, 2829-516 Caparica, Portugal*
[c] *Department of Clinical Chemistry, Free University Medical Center, De Boelelaan 1117, 1081 HV Amsterdam, The Netherlands*
[d] *Laboratory Genetic Metabolic Diseases, Department of Clinical Chemistry and Pediatrics, Academic Medical Centre, University of Amsterdam, Meibergdreef 9, 1105 AZ Amsterdam, The Netherlands*

Received 28 May 2008; revised 6 August 2008; accepted 22 August 2008

Available online 5 September 2008

Edited by Judit Ovádi

Abstract The pyruvate uptake rate in inverted submitochondrial vesicles prepared from rat liver was optimized and further characterized; the potential inhibitory effects of the anticonvulsive drug valproic acid or 2-*n*-propyl-pentanoic acid (VPA), Δ^4-valproic acid or 2-*n*-propyl-4-pentenoic acid and the respective coenzyme A (CoA) conjugates were studied in the presence of a proton gradient. All tested VPA metabolites inhibited the pyruvate uptake, but the CoA esters were stronger inhibitors (40% and 60% inhibition, respectively, for valproyl-CoA and Δ^4-valproyl-CoA, at 1 mM). At the same concentration, the specific inhibitor 2-cyano-4-hydroxycinnamate decreased the pyruvate uptake rate by 70%. The reported inhibition of the mitochondrial pyruvate uptake may explain the significant impairment of the pyruvate-driven oxidative phosphorylation induced by VPA.

Keywords: Valproic acid; Δ^4-Valproic acid; Mitochondrial pyruvate uptake; Pyruvate transport; Drug metabolism; Inverted submitochondrial membranes

1. Introduction

The oxidative metabolism of pyruvate in mitochondria is a highly regulated process which depends on the import and/or diffusion of this 2-oxoacid from the cytosolic compartment. Any xenobiotic that may interfere with this transport will compromise mitochondrial functioning and thus energy metabolism. Valproic acid (VPA, 2-*n*-propyl-pentanoic acid) is a powerful antiepileptic drug, with specific indications for many forms of epilepsy and many types of seizures, affecting children or adults.

*Corresponding author. Fax: +351 21 794 64 91.
E-mail address: mbsilva@ff.ul.pt (M.F.B. Silva).

Abbreviations: VPA, valproic acid or 2-*n*-propyl-pentanoic acid; Δ^4-VPA, Δ^4-valproic acid or 2-*n*-propyl-4-pentenoic acid; CoA, coenzyme A; VP-CoA, valproyl-CoA; Δ^4-VP-CoA, Δ^4-valproyl-CoA; ISMV, inverted submitochondrial vesicles; IMM, inner mitochondrial membrane; UCP, uncoupling protein; CHC, 2-cyano-4-hydroxycinnamate; SEM buffer, sucrose/EGTA/MOPS buffer; MES, 2-[*N*-morpholino]ethanesulfonic acid; HEPES, *N*-(2-hydroxyethyl)piperazine-*N*′-(2-ethanesulfonic acid); DCIP, 2,6-dichloroindophenol

Previous in vitro studies from our group showed that VPA and its metabolites induce a striking decrease in the pyruvate-driven mitochondrial oxygen consumption and ATP synthesis [1]. One hypothesis raised by these results was the putative interference of VPA or its biotransformation products with the mitochondrial pyruvate uptake. Besides its complete oxidation, the transport of pyruvate across mitochondrial membranes is an essential process for many other metabolic pathways, such as glucose oxidation, lipogenesis, gluconeogenesis and amino acid metabolism [2].

Since the early 1970s, many proteins that transport metabolites, nucleotides and co-factors across the inner mitochondrial membrane (IMM) have been identified [3]. The mitochondrial ADP/ATP carrier, the uncoupling proteins (UCPs), the phosphate, oxoglutarate/malate, citrate and carnitine/acylcarnitine carriers among many others, have been identified, purified and characterized [3,4].

The transport of pyruvate was first described by Papa et al. in 1971, in rat liver mitochondria, and it was shown that this process is coupled to proton symport [5]. Later, in 1974, Halestrap and Denton identified a potent and specific inhibitor of pyruvate transport, i.e. 2-cyano-4-hydroxycinnamate (CHC) suggesting the existence of a specific carrier involved in the pyruvate transport across the IMM [6–10].

The transport of pyruvate in bovine heart mitochondria was also characterized [11] and the transport assays were performed using a reconstituted system of solubilized submitochondrial particles incorporated into liposomes [11,12]. Using this system, the CHC-sensitive pyruvate-exchange reaction had substrate and inhibitor characteristics similar to those observed in mitochondria. A 34 kDa protein was described as being responsible for the pyruvate uptake both in bovine heart [11] and rat liver mitochondria [13]. In yeast, the pyruvate carrier was identified in a fraction containing two polypeptides of apparent molecular mass of 26 and 50 kDa [14].

In 2003, Hildyard et al. identified the mitochondrial pyruvate carrier in *Saccharomyces cerevisiae*, by measuring the inhibitor-sensitive pyruvate uptake in isolated mitochondria from mutant yeast strains in which the genes coding for each of the members of the mitochondrial carrier family, were disrupted one-by-one [2,15]. Mitochondria isolated from the yeast mutant YIL006w exhibited a specific loss of pyruvate uptake. However, the gene product of YIL006w, named Ndt1p, was

0014-5793/$34.00
doi:10.1016/j.febslet.2008.08.028

later shown to transport NAD^+ instead of pyruvate [16] which casts doubt about the function of this protein as a mitochondrial pyruvate carrier in yeast.

In plants, several biochemical and molecular studies have suggested the presence of a specific carrier in the IMM which mediates the electroneutral uptake of pyruvate, driven by a pH gradient. This protein was found to be inhibited by CHC and other molecules, giving support to the fact that (1) plant pyruvate transport has biochemical features similar to mammalian pyruvate transport and that (2) it involves a carrier rather than pyruvate entering by means of diffusion [17].

The UCPs are also specialized transporters located in the IMM. They allow passive proton transport through the IMM, reducing the proton electrochemical gradient built up by the respiratory chain [18,19]. Different isoforms of these proteins have been identified in mammals (UCP1 present in brown adipocytes, UCP2 in several tissues, UCP3 in brown adipose tissue and muscle, UCP4 and UCP5 in brain) [19]. Moreover, it has been reported that UCP1 exhibits the widest substrate specificity among the other homologous anion transporters, being also able to transport pyruvate [20]. The liver is the organ in which expression of UCPs is the lowest, at least under basal conditions [21]. Only a low level of expression of UCP2 was detected in the adult rat liver [21], as other UCP genes are silent in this tissue.

The hypothesis that the mitochondrial pyruvate uptake could be affected by VPA, has been proposed in one single study, using brain mitochondria [22] where a competitive inhibition mechanism was reported. Nevertheless, under in vivo conditions VPA will probably undergo rapid activation to its coenzyme A (CoA)-ester and will also be metabolized. This prompted the study described in this paper, in which we studied the effect of VPA and the respective CoA-ester [23,24], as well as Δ^4-valproic acid or 2-*n*-propyl-4-pentenoic acid (Δ^4-VPA), its main microsomal product [25], and Δ^4-valproyl-CoA (Δ^4-VP-CoA) [26]. The results presented herein provide evidence that VPA, and in particular some specific metabolites that are most probably more abundant in cytosol and/or mitochondria than the parent molecule [24], inhibit the uptake of pyruvate in inverted submitochondrial vesicles (ISMV), accounting for the mitochondrial dysfunction that has been associated with valproate.

2. Materials and methods

2.1. Materials

Sucrose, BSA, CHC, valinomycin, L-lactate, VPA and other chemicals were obtained from SIGMA® Aldrich. The sodium salt of [1-^{14}C]-pyruvic acid (250 μCi, specific activity 27 mCi/mmol, 243 μCi/mg, M = 111 g/mol) was obtained from Amersham Biosciences. Ultima-Gold® liquid scintillation solution was purchased from Packard.

2.2. Synthesis of valproyl-CoA (VP-CoA), Δ^4-VPA and Δ^4-VP-CoA

VP-CoA and Δ^4-VP-CoA were synthesized according to published procedures [24] from VPA and Δ^4-VPA, respectively. Δ^4-VPA was obtained by chemical synthesis following a reported procedure [27]. VP-CoA and Δ^4-VP-CoA were purified by solid phase extraction, and its purity checked using HPLC with diode array detection (>95%).

2.3. Isolation of rat liver mitochondria

The study was conducted according to the National Guidelines for the care and use of laboratory animals (Faculty of Pharmacy animals' laboratory).

Adult male Wistar rats (200–300 g) were starved for 18–20 h. After cervical displacement, the livers were immediately removed and rinsed into ice-cold homogenization medium containing 250 mM sucrose, 0.5 mM ethylene glycol-bis(β-aminoethyl ether)-*N*,*N*,*N*′,*N*′-tetraacetic acid, 5 mM 3-[*N*-morpholino]propanesulfonic acid, pH 7.4 (sucrose/EGTA/MOPS buffer, SEM buffer). Rat liver mitochondria were prepared according to a published procedure [24]. Briefly, after mincing and 2–3 washings with SEM buffer (at 4 °C), the chopped liver was homogenized in a precooled Teflon pestle glass homogenizer. From here onwards the whole process was conducted at 4 °C. The homogenate was centrifuged at $600 \times g$ (10 min) and the obtained post-nuclear supernatant was further centrifuged at $3600 \times g$ (10 min). The obtained pellet was suspended in SEM buffer and after one last round of centrifugation at $2700 \times g$ (10 min), the mitochondria were finally resuspended in the homogenization medium (25–50 mg/ml).

2.4. Preparation of ISMV

ISMV were obtained from the above prepared rat liver mitochondria according to a published procedure [28] with minor modifications. Mitochondria were resuspended in 0.25 M sucrose and 1 g/l BSA keeping the temperature at 4 °C. The suspension was gently homogenized with a dounce tissue grinder (6–7 strokes) and centrifuged at $27\,000 \times g$ (15 min). The obtained pellet was resuspended in 5 ml of sonication medium (225 mM sucrose, 10 mM NaH_2PO_4, 1 g/l BSA, pH 7.4) and sonicated 3×30 s. The obtained vesicle suspension was diluted in 25 ml of sonication medium and centrifuged at $23\,500 \times g$ (10 min). The supernatant was further centrifuged at $44\,000 \times g$ (60 min). The ISMV were obtained after resuspending the final pellet in 2 ml of a medium containing 225 mM sucrose, 10 mM Tris–HCl, 1 mM EDTA and 1 g/l BSA (pH 7.4) and passing it through a 21 g needle. Protein was measured using the Bradford method [29], with BSA as a reference substance. This sonication technique provides an homogeneously oriented vesicle preparation with a percentage of inversion ranging from 90% to 96% [28,30].

2.5. Characterization of ISMV preparations

2.5.1. Succinate dehydrogenase activity. The purity of the membrane vesicle preparation was assessed by the measurement of succinate dehydrogenase activity as described elsewhere [31]. The reaction mixture contained 50 mM KPi, 0.015% 2,6-dichloroindophenol (DCIP), 2 mM KCN and 15 mM sodium succinate. Reactions were started by adding 50 μl of sample (approx. 40 μg of protein) and the decrease in absorbance was measured at 600 nm (total volume 1 ml). The enzyme activity was calculated using $\varepsilon_{\mathrm{DCIP}\,600\,\mathrm{nm}} = 21\ \mathrm{mM}^{-1}\ \mathrm{cm}^{-1}$.

2.5.2. Vesicle size determination. Vesicle size of all prepared batches was determined by quasi-elastic light scatter (QELS) using a particle sizer (BI-90 Brookhaven Instruments). An application of this technique in the determination of vesicular sizes has been published [32].

2.5.3. Osmotic response by stopped-flow light-scatter. In order to assure the sealing and leakiness of the membrane vesicles, the osmotic response of ISMV (swelling and shrinking) was assessed by stopped-flow light scattering in which aliquots of ISMV were subjected to hypo- and hyperosmotic shocks. Experiments were performed on a HI-TECH Scientific PQ/SF-53 stopped-flow apparatus, which has a 2 ms dead time, interfaced with an IBM PC/AT compatible 80386 microcomputer, at a controlled temperature. ISMV in the isotonic resuspension buffer (0.1 ml, 0.4 mg/ml protein) were mixed with an equal amount of hypo-, iso- or hyper-osmotic mannitol solutions at 23 °C to reach different inwardly or outwardly directed gradients of solute (swelling and shrinking; osmotic gradients −62.5, 0, 125 and 375 mosM). The time-course of 90° scattered light intensity at 400 nm was followed until a stable light-scattered signal was obtained. The change in light scatter intensity (I) of the ISMV preparation after an osmotic shock ($\Delta I = I_0 - I_\infty$) is related to their vesicular volume change [33] and thus, it can be used as a tool to assure vesicle integrity. The osmolarities of all solutions were measured using a cryometric automatic semi-micro osmometer (Knauer, Germany).

2.6. Pyruvate uptake measurements

The rate of the radiolabeled substrate [1-^{14}C]-pyruvate uptake by ISMV was measured in the presence or absence of an inwardly directed proton gradient. Prior to the uptake, the ISMV were equilibrated in 100 mM KCl, 20 mM *N*-(2-hydroxyethyl)piperazine-*N*′-(2-ethanesulfonic acid) (HEPES), pH 7.4, by passing the vesicle preparation

through a 21 g needle. The mitochondrial proton driven pyruvate uptake was measured at 4 °C after incubation of the ISMV suspension (final concentration range: 0.1–5.7 mg/ml, pH 7.4) with 5 µl of 240 mM 2-[*N*-morpholino]ethanesulfonic acid (MES) containing 0.066 µCi of [1-^{14}C]-pyruvate and 10 µM valinomycin, resulting in an extravesicular pH of 5.5 and a final concentration of 0.02–0.67 mM pyruvate (final volume: 30 µl). The reaction was stopped by diluting the sample with ice-cold stop solution (84 mM KCl, 17 mM HEPES, 40 mM MES, 1 mM CHC, pH 5.5) at appropriate times (0–60 s), followed by rapid filtration in a vacuum assembly through Osmonics filters (0.45 µm pore size), and 2–3 washing steps with the same cold stop solution [34]. The filters were dried at room temperature, and the vesicle-associated radioactivity in the filters was determined by liquid scintillation counting in a Packard Tri-Carb 2100 TR Liquid Scintillation Analyzer. The non-specific binding of the isotope to the surface of the vesicles as well as to the filters was determined by a similar pyruvate uptake experiment but without incubation. An average value was obtained from triplicate measurements (blanks), which was subtracted in further corresponding experiments.

Pyruvate exchange in the absence of a proton gradient was assayed under similar experimental conditions, replacing the incubation medium by 100 mM KCl, 20 mM HEPES containing [1-^{14}C]pyruvate and 10 µM valinomycin, resulting in an extravesicular pH of 7.4. The stop solution consisted of 100 mM KCl, 20 mM HEPES and 1 mM CHC, final pH 7.4, and the subsequent steps were performed accordingly.

2.7. Pyruvate uptake measurements in the presence of inhibitors

The effect of VPA, VP-CoA, Δ^4-VPA and Δ^4-VP-CoA on the mitochondrial pyruvate uptake was assessed by pre-incubating the ISMV (2 mg/ml) with purified solutions of these compounds at various concentrations (0.5–2 mM), for 3 min, prior to the uptake assay. CHC, a powerful and specific inhibitor of the mitochondrial pyruvate carrier [8], was used as a positive control. The effect of lactate was also studied using a similar concentration range. The subsequent pyruvate uptake measurement driven by an inwardly directed proton gradient was assayed as described above, incubating the vesicles for 5 s with [1-^{14}C]-pyruvate at various concentrations (0.07, 0.17 and 0.67 mM final concentrations).

2.8. Data analysis

The kinetic parameters of the mitochondrial pyruvate transport activity were determined by non-linear regression analysis using the SigmaPlot® 9.0 Technical Graphing Software.

3. Results

3.1. Characterization of the inner ISMV

Purified ISMV were prepared from mitochondria isolated from rat liver homogenates by differential centrifugation. The activity of the marker enzyme succinate dehydrogenase, an enzymatic complex bound to the IMM that participates in both the citric acid and the mitochondrial electron transport chain (complex II), was measured. The obtained values were 0.013 ± 0.002 U/mg protein and 0.023 ± 0.01 U/mg protein, respectively, determined in the initial mitochondrial homogenates and in the ISMV suspension, indicating a two-fold vesicle enrichment after purification.

The size distribution of ISMV preparations determined by quasi-elastic light scattering is shown in Fig. 1A. A mean diameter

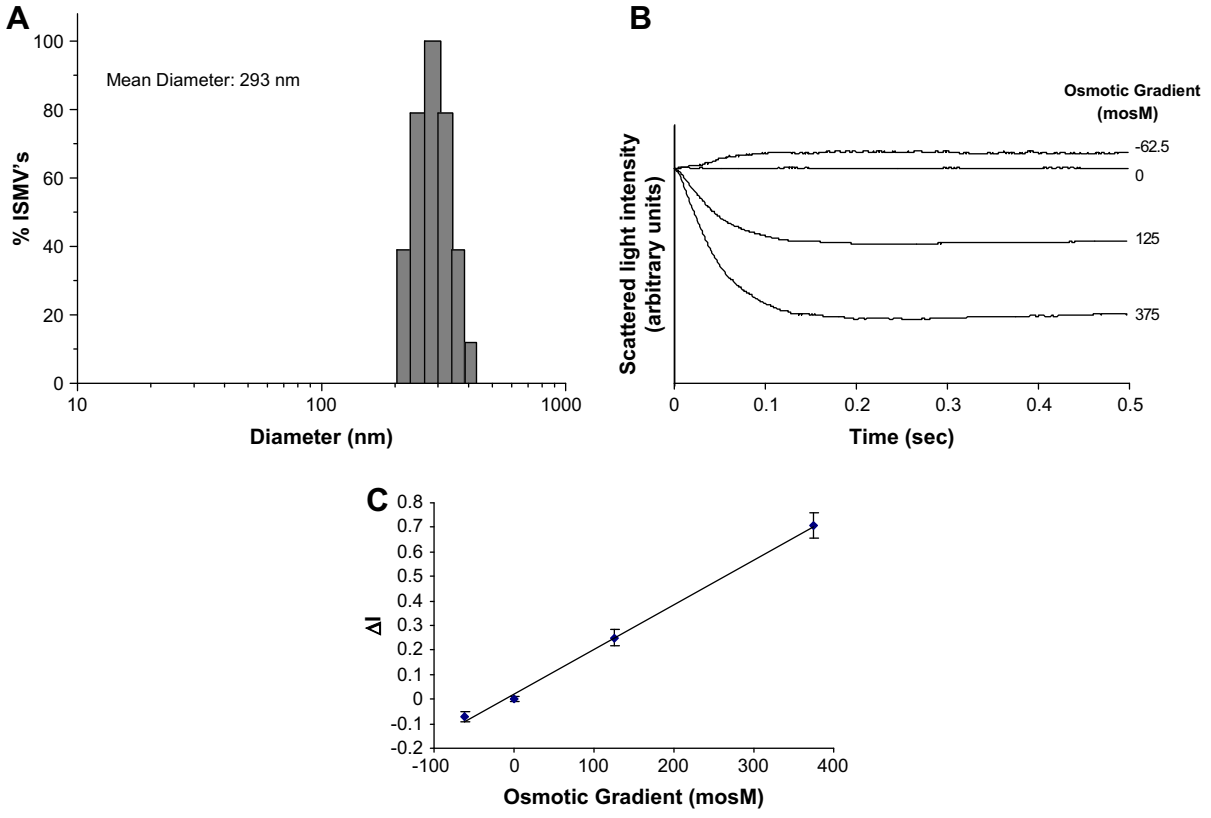

Fig. 1. (A) ISMV size determination by quasi-elastic light scattering (QELS). Vesicles in the resuspension buffer were homogeneous in size with a mean diameter of 293 ± 12 nm (n = 10). (B) Record of a typical stopped-flow experiment where the light scatter intensity from an ISMV suspension was suddenly exposed to different osmotic shocks (−62.5, 0, 125 and 375 mosM). The time course of volume change was followed for 0.5 s. (C) Dependence of the total change in light scatter ($\Delta I = I_0 - I_\infty$), related to the total volume change of the ISMV vesicles, for a specific applied osmotic gradient (mosM).

value of 293 ± 12 nm was obtained in the prepared batches ($n = 10$) and as depicted, a unimodal distribution was achieved, demonstrating that the vesicles were homogeneous in size.

Fig. 1B shows the recordings of a typical stopped-flow experiment where the light scatter intensity from an ISMV suspension suddenly exposed to different solutions (iso-, hyper- and hypo-osmotic) was monitored for 0.5 s. A remarkable increase in scattered light was observed when vesicles were subjected to hyper-osmotic gradients of 125 and 375 mosM, in contrast to the light scatter decrease for the hypo-osmotic gradient −62.5 mosM, in agreement with vesicle shrinking and swelling. No change in scattered light was observed when vesicles were mixed with iso-osmotic buffer (absence of osmotic gradient). The dependence of the total change in light scatter (ΔI) for a given osmotic gradient applied (mosM) is shown in Fig. 1C and demonstrates that the vesicles behaved like osmometers for the chosen osmolarity range, therefore assuring vesicle integrity.

3.2. Pyruvate uptake measurements in ISMV

3.2.1. Time course and substrate dependence. Pyruvate uptake was assayed in vitro using purified ISMV by measuring the uptake of [1-^{14}C]-pyruvate by these vesicles. The rate of labelled substrate accumulation inside the vesicles was measured through a rapid filtration technique and isotope scintillation counting.

As shown in Fig. 2, a time-dependent uptake of radiolabeled pyruvate was observed in ISMV, in the presence of an inwardly directed proton gradient (pH_{out} 5.5 < pH_{in} 7.4) suggesting apparent first order kinetics. Moreover, virtually no pyruvate uptake was observed in the absence of a proton gradient ($pH_{out} = pH_{in}$ 7.4). The rate of pyruvate uptake in the prepared vesicles was linearly dependent on the protein content (0–6 mg/ml, data not shown). Considering the above results, a reaction time of 5 s and a protein content of 2 mg/ml were selected for all subsequent studies.

The concentration dependence of pyruvate uptake was also studied in ISMV, in the presence and absence of a driving proton gradient. Fig. 3 shows the uptake rate as function of the pyruvate concentration. From a double reciprocal plot and

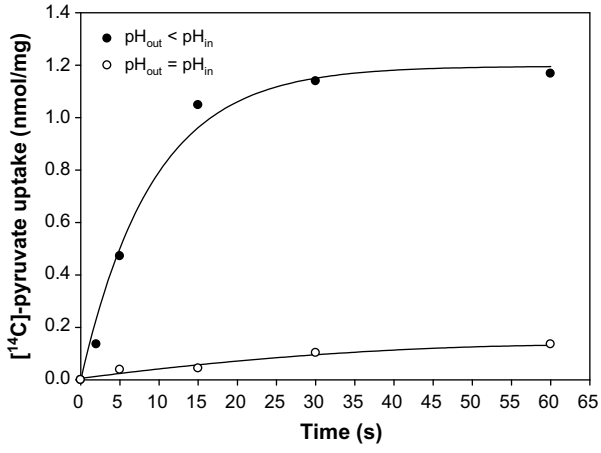

Fig. 2. Uptake of [^{14}C]-pyruvate by ISMV driven by an inwardly directed proton gradient ($pH_{out} < pH_{in}$) (closed circles ●), and without proton gradient ($pH_{out} = pH_{in}$) (opened circles ○). The data shown correspond to mean of triplicates (S.D. < 0.03) obtained in two independent experiments.

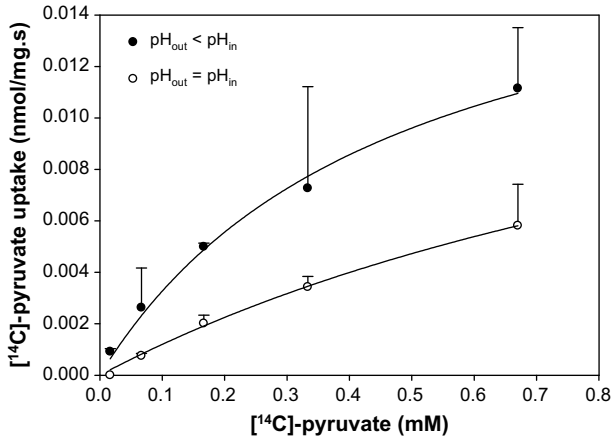

Fig. 3. Effect of the proton gradient in the pyruvate uptake in ISMV as function of increasing substrate concentration. The uptake was driven by an inwardly directed proton gradient ($pH_{out} < pH_{in}$) (closed circles ●), and without proton gradient ($pH_{out} = pH_{in}$) (opened circles ○). The data shown are mean ± S.D. of triplicates of two independent experiments.

from a non-linear regression analysis using the SigmaPlot® 9.0 Technical Graphing Software, values of K_m and V_{max} were obtained and are presented in Table 1. In the presence of a proton gradient, an approximate K_m of 0.48 mM was calculated, a value much lower than the value of 1.40 mM obtained in the absence of a proton gradient. These values suggest an increase in substrate affinity of the mediated pyruvate transport when a proton force is driving the uptake. The V_{max} was 5.5% higher in the presence of a proton gradient.

3.2.2. Inhibitory effect of different VPA metabolites on the uptake of [^{14}C]-pyruvate. Fig. 4 shows the [^{14}C]-pyruvate uptake in ISMV in the presence of CHC, VPA, Δ^4-VPA and the respective CoA esters (VP-CoA and Δ^4-VP-CoA).

The parent drug, VPA, and its unsaturated metabolite, Δ^4-VPA (both at 1 mM), had only a mild to insignificant effect on the mitochondrial uptake of pyruvate (22.0% and 15.7% inhibition, respectively). However, at a higher concentration (2 mM) only Δ^4-VPA induced a significant inhibition of the pyruvate uptake rate (76.2% inhibition), as shown in Fig. 4A.

Furthermore, the uptake of pyruvate was also found to be inhibited by both Δ^4-VP-CoA (73.1% inhibition) and VP-CoA (50.1% inhibition), in parallel with an increase of K_m values for the pyruvate transport (Fig. 4B and Table 1).

Our results confirm, by comparing all the tested compounds at 1 mM, that CHC was in fact an effective inhibitor of the pyruvate uptake in ISMV (71.6% inhibition), as shown in Fig. 4B and C.

Lactate, a substrate that potentially competes with pyruvate, also inhibited this ketoacid uptake in ISMV (42.1% inhibition) as depicted in Fig. 4A and C.

Table 1 summarises the kinetic parameters values of the pyruvate uptake, calculated in the presence of the tested VPA metabolites, CHC and lactate, as well as the obtained inhibition (%) of control uptake values.

4. Discussion

The transport of pyruvate across membranes plays a central role in cellular metabolism and metabolic communication be-

Table 1
Effect of different inhibitors on the mitochondrial pyruvate uptake in ISMV

Kinetic parameters[a]	$pH_{out} = pH_{in}$	$pH_{out} < pH_{in}$						
	Control	Control	VPA[b]	VP-CoA[c]	Δ^4-VPA[c]	Δ^4-VP-CoA[c]	CHC[b]	Lactate[b]
K_m	1.40	0.48	–	–	–	–	–	–
K_m^{app}	–	–	0.47	0.64	0.95	1.02	–	–
V_{max}	17.90	18.88	–	–	–	–	–	–
V_{max}^{app}	–	–	17.89	22.29	16.29	22.82	–	–
Inhibition (%)	–	–	22.0	50.1	76.2	73.1	71.6	42.1

The values represent the apparent kinetic parameters (K_m^{app} and V_{max}^{app}) and the average value of maximum inhibition (%) of the pyruvate uptake (100 minus % of control) in the presence of the respective inhibitors. Data shown are mean ± S.D. of triplicates of at least two independent experiments.
[a]Values of K_m and V_{max} are, respectively, expressed in mM and pmol/mg s.
[b][Inhibitor] = 1 mM.
[c][Inhibitor] = 2 mM.

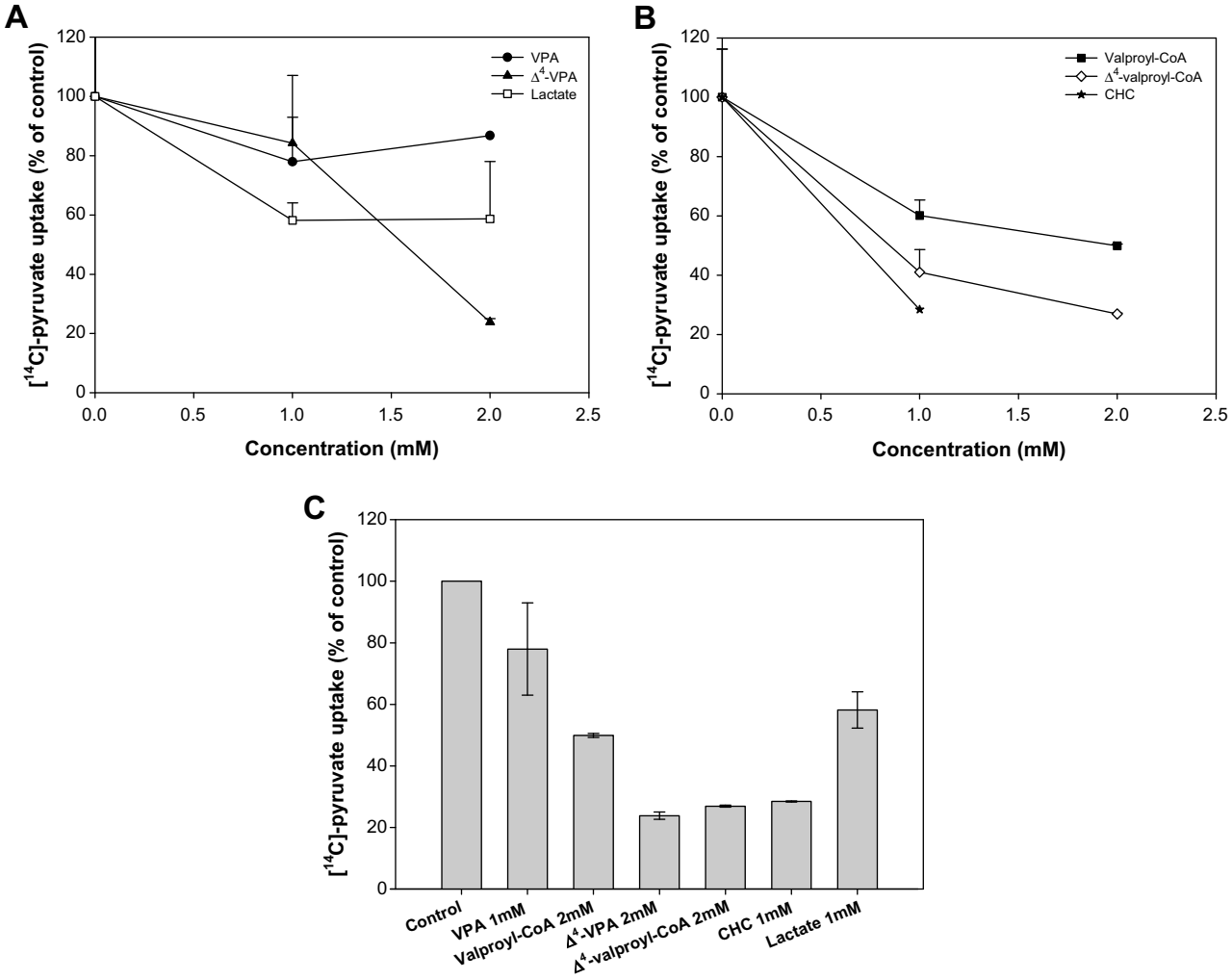

Fig. 4. [^{14}C]-pyruvate uptake in ISMV using a proton gradient, in the presence of (A) valproic acid (VPA), Δ^4-VPA and lactate and (B) valproyl-CoA, Δ^4-valproyl-CoA and 2-ciano-4-hydroxycinnamate (CHC). (C) Maximum inhibition of the pyruvate uptake obtained with the different VPA metabolites, compared with the control (100% of pyruvate uptake obtained in the absence of inhibitors) and the specific pyruvate carrier inhibitor CHC (28% of pyruvate uptake). Data shown are mean ± S.D. of triplicates of at least two independent experiments.

tween subcellular compartments and tissues [15,35,36]. Many cells rely on the end product of glycolysis, i.e. pyruvate, to produce most of their ATP. This pathway occurs in the cell cytosol, and thus the transport of pyruvate into the mitochondria for further oxidation, is essential to fuel the citric acid cycle after being converted into acetyl-CoA by pyruvate dehydrogenase [35,36]. For this purpose, the mitochondrial pyruvate carrier activity is critical for energy homeostasis.

The transport of monocarboxylates, such as pyruvate and lactate across the plasma membrane is well-characterized and catalysed by a recently identified family of proton-linked monocarboxylate transporters [36]. In mitochondria, the mammalian pyruvate carrier has not yet been cloned, sequenced and fully characterized, however, it has been considered as a member of the six-transmembrane-helix mitochondrial carrier family [15].

After the identification of CHC as a specific and potent inhibitor of the putative mitochondrial pyruvate carrier [6,9], the existence of such protein has gained support by many studies and recently new highly potent inhibitors have been identified [15,35,36].

The scope of this paper is primarily focused on functional studies using a simple experimental model to test the direct effect of a specific drug and/or its metabolites on the mitochondrial uptake of pyruvate. This study was performed using ISMV, which allowed a strict control of the driving force of pyruvate uptake, by regulating both internal and external pH. Furthermore, the approach was strictly focused on the proton-dependent transport of pyruvate and no other internal substrates were added, excluding other putative pyruvate translocators. The former uptake experiments using intact mitochondria and labelled pyruvate could not avoid the subsequent metabolism of the substrate inside the organelle, a fact that would certainly affect the pH and the osmolarity in the matrix. The obtained homogeneity of the prepared ISMV either in size or orientation, accounts for reproducible kinetic measurements, at controlled conditions of pH.

Using this model, the results presented in this paper show that pyruvate uptake decreases in ISMV in the absence of a driving proton gradient, suggesting that the mitochondrial transport of pyruvate is protein-mediated and coupled with a proton-symport, as already proposed [2,36]. In addition, CHC significantly inhibited the uptake of this monocarboxylate in the prepared vesicles, supporting the previous hypothesis. Furthermore, the uptake of pyruvate was inhibited in the presence of lactate, suggesting that this compound may compete with pyruvate into these vesicles.

In the present study, VPA and Δ^4-VPA were found to clearly inhibit the uptake of pyruvate in ISMV (as indicated by the observed increase on the K_m for pyruvate uptake). In addition, our results suggest that the respective CoA esters of VPA and Δ^4-VPA are stronger inhibitors of the mitochondrial pyruvate uptake than the parent drug (VPA). Both free acids were recently found to be activated to the respective CoA esters not only at the mitochondrial matrix, where the free acids are prone to be metabolized by β-oxidation in the form of CoA esters, but also in the extra-mitochondrial compartment [26]. The extra-mitochondrial formation of VP-CoA and Δ^4-VP-CoA may affect numerous cellular functions, such as fatty-acid elongation, peroxisomal metabolism, gluconeogenesis, ureagenesis and many other pathways involving cytosolic reactions. A targeted effect of these CoA conjugates on the mitochondrial pyruvate uptake is the hypothesis clearly supported by the present results.

Previous studies of our group have shown that oxygen consumption and ATP synthesis driven by pyruvate was severely decreased by VPA [1]. In addition, we recently reported that VPA and Δ^4-VPA also inhibit both 2-oxoglutarate and glutamate-driven oxidation and ATP synthesis [37] although not so strikingly as with pyruvate. The reported data suggest that the observed inhibitory effects of VPA and metabolites on mitochondrial ATP synthesis and oxidation of pyruvate, 2-oxoglutarate and glutamate are likely due to an inhibitory effect on dihydrolipoamide dehydrogenase (DLDH, E_3 subunit), the common component of the multi-enzyme complexes 2-oxoglutarate dehydrogenase, pyruvate dehydrogenase and branched-chain 2-oxoacid dehydrogenase [37]. However, a specific effect on the transport systems in the mitochondrial inner membrane could not be excluded. Thus, the defective import of pyruvate into this organelle suggested by the present results mainly induced by the respective CoA-esters (VP-CoA and Δ^4-VP-CoA), would be additive to the reported DLDH inhibition. Being structurally related, those CoA esters do not diffuse in membranes, due to their larger size and presence of double bounds, and thereby they can potentially affect pyruvate uptake by interfering with the substrate binding-site or by modifying the protein transporter properties. Considering the free acids, the data presented in this work suggest that the monocarboxylate anions, valproate and Δ^4-valproate might enter into the mitochondrial matrix by a symport process with H^+, competing with pyruvate for the same proton-linked transporter. However, further studies are required in order to elucidate the mechanisms of the reported inhibition on the mitochondrial uptake of pyruvate.

The present data do clearly support an inhibition of the mitochondrial CHC-sensitive pyruvate/H+ symporter by VPA and its derivatives. However, the efficacy of other potential pyruvate uptake mechanisms, such as UCP1 and/or other CHC-insensitive antiporter mechanisms [38–40] which may (or may not) be inhibited by this drug, can possibly obviate a net reduction in pyruvate transport in vivo.

The conversion of pyruvate to glucose, involving firstly its uptake into mitochondria, is a crucial pathway in liver metabolism and a clear inhibition of gluconeogenesis from both lactate and pyruvate by VPA and Δ^4-VPA has long been recognized [41,42]. The influence of VPA on carbohydrate metabolism is undisputed, since a significant weight-gain is the most frequently reported adverse effect of a long-term VPA treatment [43,44], potentially associated with hyperinsulinemia and steatosis. In addition, the effects of the drug on fatty acid oxidation are well-documented [45] but their consequences to the imbalance of glucose homeostasis are far from being elucidated, considering the reciprocally linked mechanisms of lipid and carbohydrate regulation in vivo.

Taken together, the present results may account for the limited oxidation of pyruvate previously observed, and thus to the compromised energy production driven by this substrate induced by VPA and/or metabolites.

Acknowledgments: This work was financially supported by Fundação para a Ciência e a Tecnologia (FCT), Lisboa, Portugal (POCTI/FCB/48800/2002 with partial funding of FEDER and SFRH/BD/22420/2005).

References

[1] Silva, M.F.B., Ruiter, J.P.N., IJlst, L., Jakobs, C., Duran, M., de Almeida, I. Tavares and Wanders, R.J.A. (1997) Valproate inhibits the mitochondrial pyruvate-driven oxidative phosphorylation in vitro. J. Inherit. Metab. Dis. 20, 397–400.

[2] Hildyard, J.C.W. and Halestrap, A.P. (2003) Identification of the mitochondrial pyruvate carrier in *Saccharomyces cerevisiae*. Biochem. J. 374, 607–611.

[3] Palmieri, F., Agrimi, G., Blanco, E., Castegna, A., Di Noia, M.A., Iacobazzi, V., Lasorsa, F.M., Morobbio, C.M.T., Palmieri, L., Scarcia, P., Todisco, S., Vozza, A. and Walker, J. (2006) Identification of mitochondrial carriers in *Saccharomyces cerevisiae* by transport assay of reconstituted recombinant proteins. Biochim. Biophys. Acta 1757, 1249–1262.
[4] Palmieri, F., Bisaccia, F., Capobianco, L., Dolce, V., Fiermonte, G., Iacobazzi, V., Indiveri, C. and Palmieri, L. (1996) Mitochondrial metabolite transporters. Biochim. Biophys. Acta 1275, 127–132.
[5] Papa, S., Francavilla, A., Paradies, G. and Meduri, B. (1971) The transport of pyruvate in rat liver mitochondria. FEBS Lett. 12 (5), 285–288.
[6] Halestrap, A.P. and Denton, R.M. (1974) Specific inhibition of pyruvate transport in rat liver mitochondria and human erythrocytes by α-cyano-4-hydroxycinnamate. Biochem. J. 138, 313–316.
[7] Halestrap, A.P. (1975) The mitochondrial pyruvate carrier: kinetics and specificity for substrates and inhibitors. Biochem. J. 148, 85–96.
[8] Halestrap, A.P. and Denton, R.M. (1975) The specificity and metabolic implications of the inhibition of pyruvate transport in isolated mitochondria and intact tissue preparations by α-cyano-4-hydroxycinnamate and related compounds. Biochem. J. 148, 97–106.
[9] Halestrap, A.P. (1976) The mechanism of the inhibition of the mitochondrial pyruvate transporter by α-cyanocinnamate derivates. Biochem. J. 156, 181–183.
[10] Halestrap, A.P. (1978) Pyruvate and ketone-body transport across the mitochondrial membrane: exchange properties, pH dependence and mechanism of the carrier. Biochem. J. 172, 377–387.
[11] Nalecz, K.A., Bolli, R., Wojtczak, L. and Azzi, A. (1986) The monocarboxylate carrier from bovine heart mitochondria: partial purification and its substrate-transporting properties in a reconstituted system. Biochim. Biophys. Acta 851, 29–37.
[12] Bolli, R., Nalecz, K.A. and Azzi, A. (1989) Monocarboxylate and α-ketoglutarate carriers from bovine heart mitochondria. J. Biol. Chem. 264 (30), 18024–18030.
[13] Capuano, F., Paola, M.D., Azzi, A. and Papa, S. (1990) The monocarboxylate carrier from rat liver mitochondria: purification and kinetic characterization in a reconstituted system. FEBS Lett. 261 (1), 39–42.
[14] Nalecz, M.J., Nalecz, K.A. and Azzi, A. (1991) Purification and functional characterisation of the pyruvate (monocarboxylate) carrier from baker's yeast mitochondria (*Saccharomyces cerevisiae*). Biochim. Biophys. Acta 1079, 87–95.
[15] Sugden, M.C. and Holness, M.J. (2003) Trials, tribulations and finally, a transporter: the identification of the mitochondrial pyruvate transporter. Biochem. J., 374, 10.1042/BJ20031105.
[16] Todisco, S., Agrimi, G., Castegna, A. and Palmieri, F. (2006) Identification of the mitochondrial NAD^+ transporter in *Saccharomyces cerevisiae*. J. Biol. Chem. 281 (3), 1524–1531.
[17] Laloi, M. (1999) Plant mitochondrial carriers: an overview. Cell. Mol. Life Sci. 56, 918–944.
[18] Criscuolo, F., Mozo, J., Hurtaud, C., Nubel, T. and Bouillaud, F. (2006) UCP2, UCP3, avUCP, what do they do when proton transport is not stimulated? Possible relevance to pyruvate and glutamine metabolism. Biochim. Biophys. Acta 1757, 1284–1291.
[19] Sluse, F.E., Jarmuszkiewicz, W., Navet, R., Douette, P., Mathy, G. and Sluse-Goffart, C.M. (2006) Mitochondrial UCPs: new insights into regulation and impact. Biochim. Biophys. Acta 1757, 480–485.
[20] Jezek, P. and Borecky, J. (1998) Mitochondrial uncoupling protein may participate in futile cycling of pyruvate and other monocarboxylates. Am. J. Physiol. Cell Physiol. 275, 496–504.
[21] Villarroya, F., Iglesias, R. and Giralt, M. (2007) PPARs in the control of uncoupling proteins gene expression. PPAR Res. 2007, 74364.
[22] Benavides, J., Martin, A., Ugarte, M. and Valdivieso, F. (1982) Inhibition by valproic acid of pyruvate uptake by brain mitochondria. Biochem. Pharmacol. 31 (8), 1633–1636.
[23] Silva, M.F.B., Ruiter, J.P.N., Overmars, H., Bootsma, A.H., van Gennip, A.H., Jakobs, C., Duran, M., de Almeida, I. Tavares and Wanders, R.J.A. (2002) Complete β-oxidation of valproate: cleavage of 3-oxovalproyl-CoA by a mitochondrial 3-oxoacyl-CoA thiolase. Biochem. J. 362, 755–760.
[24] Silva, M.F.B., Ruiter, J.P.N., IJlst, L., Allers, P., ten Brink, H.J., Jakobs, C., Duran, M., de Almeida, I. Tavares and Wanders, R.J.A. (2001) Synthesis and intramitochondrial levels of valproyl-Coenzyme A metabolites. Anal. Biochem. 290, 60–67.
[25] Abbott, F.S. and Anari, M.R. (1999) Chemistry and biotransformation in: Milestones in Drug Therapy-Valproate (Löscher, W., Ed.), pp. 47–75, Birkhäuser Verlag, Basel.
[26] Aires, C.C.P., Ruiter, J.P.N., Luís, P.B.M., ten Brink, H.J., IJlst, L., de Almeida, I. Tavares, Duran, M., Wanders, R.J.A. and Silva, M.F.B. (2007) Studies on the extra-mitochondrial CoA-ester formation of valproic and 4-valproic acids. Biochim. Biophys. Acta 1771, 533–543.
[27] Rettenmeyer, A.W., Prickett, K.S., Gordon, W.P., Bjorge, S.M., Chang, S.-L., Levy, R.H. and Baillie, T.A. (1985) Studies on the biotransformation in the perfused rat liver of 2-*n*-propyl-4-pentenoic acid, a metabolite of the antiepileptic drug valproic acid. Evidence for the formation of chemically reactive intermediates. Drug Metab. Dispos. 13, 81–96.
[28] Hautecler, J.J., Sluse-Goffart, C.M., Evens, A., Duyckaerts, C. and Sluse, F.E. (1994) Effect of aspartate and glutamate on the oxoglutarate carrier investigated in rat heart mitochondria and inverted submitochondrial vesicles. Biochim. Biophys. Acta 1185, 153–159.
[29] Bradford, M.M. (1976) A rapid and sensitive method for the quantification of microgram quantities of protein utilizing the principle of protein-dye binding. Anal. Biochem. 72, 248–254.
[30] Harmon, H.J. (1982) Isolation of totally inverted submitochondrial particles by sonication of beef heart mitochondria. J. Bioenerg. Biomembr. 14, 377–386.
[31] King, T.E. (1967) Preparation of succinate dehydrogenase and reconstitution of succinate oxidase. Method Enzymol. 10, 322–331.
[32] Perevucnik, G., Schurtenberger, P., Lasic, D.D. and Hauser, H. (1985) Size analysis of biological membrane vesicles by gel filtration, dynamic light scattering and electron microscopy. Biochim. Biophys. Acta 821 (1), 169–173.
[33] Soveral, G., Macey, R.I. and Moura, T.F. (1997) Water permeability of brush border membrane vesicles from kidney proximal tubule. J. Membr. Biol. 158 (3), 219–228.
[34] Havelaar, A.C., Mancini, G.M.S., Beerens, C.E.M.T., Souren, R.M.A. and Verheijen, F.W. (1998) Purification of the lysosomal sialic acid transporter. J. Biol. Chem. 273 (51), 34568–34574.
[35] Hildyard, J.C.W., Ammala, C., Dukes, I.D., Thomson, S.A. and Halestrap, A.P. (2005) Identification and characterization of a new class of highly specific and potent inhibitors of the mitochondrial pyruvate carrier. Biochim. Biophys. Acta 1707, 221–230.
[36] Halestrap, A.P. and Price, N.T. (1999) The proton-linked monocarboxylate transporter (MCT) family: structure, function and regulation. Biochem. J. 343, 281–299.
[37] Luís, P.B.M., Ruiter, J.P.N., Aires, C.C.P., Soveral, G., de Almeida, I. Tavares, Duran, M., Wanders, R.J.A. and Silva, M.F.B. (2007) Valproic acid metabolites inhibit dihydrolipoyl dehydrogenase activity leading to impaired 2-oxoglutarate-driven oxidative phosphorylation. Biochim. Biophys. Acta 1767, 1126–1133.
[38] Valenti, D., de Bari, L., Atlante, A. and Passarella, S. (2002) L-Lactate transport into rat heart mitochondria and reconstruction of the L-lactate/pyruvate shuttle. Biochem. J. 364 (Pt 1), 101–104.
[39] Passarella, S., Atlante, A., Valenti, D. and de Bari, L. (2003) The role of mitochondrial transport in energy metabolism. Mitochondrion 2, 319–343.
[40] De Bari, L., Atlante, A., Valenti, D. and Passarella, S. (2004) Partial reconstruction of in vitro gluconeogenesis arising from mitochondrial L-lactate uptake/metabolism and oxaloacetate export via novel L-lactate translocators. Biochem. J. 380 (Pt. 1), 231–242.
[41] Becker, C.M. and Harris, R.A. (1983) Influence of valproic acid on hepatic carbohydrate and lipid metabolism. Arch. Biochem. Biophys. 223, 381–392.

[42] Rogiers, V., Vandenberghe, Y. and Vercruysse, A. (1985) Inhibition of gluconeogenesis by sodium valproate and its metabolites in isolated rat hepatocytes. Xenobiotica 15, 759–765.
[43] Schmidt, D. (1999) Adverse effects and interactions with other drugs in: Milestones in Drug Therapy-Valproate (Löscher, W., Ed.), pp. 223–264, Birkhäuser Verlag, Basel.
[44] El-Khatib, F., Rauchenzauner, M., Lechleitner, M., Hoppichler, F., Naser, A., Waldmann, M., Trinka, E., Unterberger, I., Bauer, G. and Luef, G.J. (2007) Valproate, weight gain and carbohydrate craving: a gender study. Seizure 16, 226–232.
[45] Silva, M.F.B., Aires, C.C.P., Luis, P.B.M., Ruiter, J.P.N., IJlst, L., Duran, M., Wanders, R.J.A. and de Almeida, I. Tavares (2008) Valproic acid metabolism and its effects on mitochondrial fatty acid oxidation: a review. J. Inherit. Metab. Dis. 31, 205–216.